Measurement of the isomer production ratio for the ^{112}Cd$(n,\gamma)^{113}$Cd reaction using neutron beams at J-PARC

T. Hayakawa,[1,2,*] Y. Toh,[3] M. Huang,[3] T. Shizuma,[1] A. Kimura,[3] S. Nakamura,[3] H. Harada,[3] N. Iwamoto,[3] S. Chiba,[4] and T. Kajino[2,5,6]

[1]*National Institutes for Quantum and Radiological Science and Technology, 2-4 Shirakata, Tokai, Naka, Ibaraki 319-1106, Japan*
[2]*National Astronomical Observatory of Japan, Mitaka, Tokyo 181-8588, Japan*
[3]*Japan Atomic Energy Agency, 2-4 Shirakata, Tokai, Naka, Ibaraki 319-1195, Japan*
[4]*Tokyo Institute of Technology, 2-12-1 Ookayama, Meguro, Tokyo 113-0033, Japan*
[5]*The University of Tokyo, Bunkyo-ku, Tokyo 113-0033, Japan*
[6]*Beihang University, Beijing 100191, China*

(Received 28 July 2016; published 15 November 2016)

The astrophysical origin of a rare isotope ^{115}Sn remains an open question. An isomer ($T_{1/2} = 14.1$ y) in ^{113}Cd is an *s*-process branching point from which a nucleosynthesis flow reaches ^{115}Sn. The *s*-process abundance of ^{115}Sn depends on the isomer production ratio in the ^{112}Cd$(n,\gamma)^{113}$Cd reaction. However, the ratio has not been measured in an energy region higher than the thermal energy. We have measured γ rays following neutron capture reactions on ^{112}Cd using two cluster high-purity germanium (HPGe) detectors in conjunction with a time-of-flight method at J-PARC. We have obtained the result that the relative γ-ray intensity ratio of the isomer is almost constant in an energy region of up to 5 keV. This result suggests that the *s*-process contribution to the solar abundance of ^{115}Sn is minor. We have found that the ratio of a resonance at 737 eV is about 1.5 times higher than other ratios. This enhancement can be explained by a *p*-wave neutron capture. This result suggests measurements of decay γ rays to isomers are effective to assign the spin and parity for neutron capture resonances.

DOI: 10.1103/PhysRevC.94.055803

I. INTRODUCTION

The astrophysical origins of neutron-deficient isotopes of ^{112,114,115}Sn were a mystery in the 1980s [1]. Most isotopes heavier than iron are synthesized by slow neutron capture reactions (*s* process) and rapid neutron capture reactions (*r* process) in stars. However, previous studies cannot explain the solar abundances of these Sn isotopes by either the *s* process or *r* process [2–6]. Figure 1 shows a partial nuclear chart and nucleosyntheses flows around Cd and Sn isotopes. The ^{112,114,115}Sn isotopes are located outside of the main flow of the *s* process and are shielded against β^- decay after the freeze-out of the *r* process by stable isobars ^{112,114}Cd and ^{115}In. Woosley *et al.* proposed nucleosyntheses by photodisintegration reactions on preexisting isotopes in supernova (SN) explosions (γ process) [7]. After this proposal, SN model calculations could explain the solar abundances of even-N isotopes of ^{112,114}Sn [7–9]. In the mass region of $50 < N < 82$ where N is the neutron number, the nucleosynthesis flow in the γ process mostly proceeds along the β-stability line [9]. Thus, the neutron-deficient isotopes such as ^{112,114}Sn are predominantly produced from heavy isotopes by successive (γ,n) reactions as shown in Fig. 1. However, γ-process model calculations alone underestimate the solar abundance of the odd-N isotope ^{115}Sn. Because the neutron thresholds of odd-N isotopes are lower than neighboring even-N isotopes, the destruction rate of an odd-N isotope by (γ,n) reactions in hot temperature environments should be larger than its production rate. Therefore, the astrophysical origin of ^{115}Sn remains an open question.

An isomer with a half-life of 14.1 yr at 264 keV in ^{113}Cd is a branching point in the *s* process, from which a nucleosynthesis flow reaches to ^{115}Sn (see the dashed arrows in Fig. 1) [1]. Hayakawa *et al.* measured the ^{112}Cd$(n,\gamma)^{113}$Cd^m reaction cross section at the thermal energy with neutrons provided from a nuclear reactor [6]. In addition, it was pointed out that the *s*-process abundance of ^{115}Sn depends on the ratio of the ^{112}Cd$(n,\gamma)^{113}$Cd^m reaction cross section to the ^{112}Cd$(n,\gamma)^{113}$Cd^{gs} reaction cross section in typical *s*-process energies of 1–50 keV. The isomer production ratio as a function of neutron energy was calculated by using a statistical model. If the isomer ratio increases suddenly in an energy region of $E > 1$ keV, the origin of ^{115}Sn may be explained by the *s* process. However, the isomer production ratio in an energy region higher than the thermal energy has not been measured.

Figure 2 shows a schematic view of neutron capture reactions on ^{112}Cd. Excited states with low spin are populated following neutron capture reactions on the $J^\pi = 0^+$ ground state of ^{112}Cd. These excited states decay away to an isomeric state with $J^\pi = 11/2^-$ or the $J^\pi = 1/2^+$ ground state of ^{113}Cd by the emission of γ rays. The maximum γ-ray energy corresponding to the neutron threshold of ^{113}Cd is about 6.54 MeV, whereas the energy difference between the ground state and the isomer is only 264 keV (see Fig. 2). Thus it is not easy to distinguish two decays to the ground state and the isomer using standard large-volume scintillation detectors. In fact, the isomer production ratios in ^{113}Cd in an energy region higher than the thermal energy have not been measured, although several measurements on Cd targets were carried out [10–12]. In the present paper, we report the relative γ-ray isomer production ratios in the ^{112}Cd(n, γ)^{113}Cd reaction using

*hayakawa.takehito@qst.go.jp

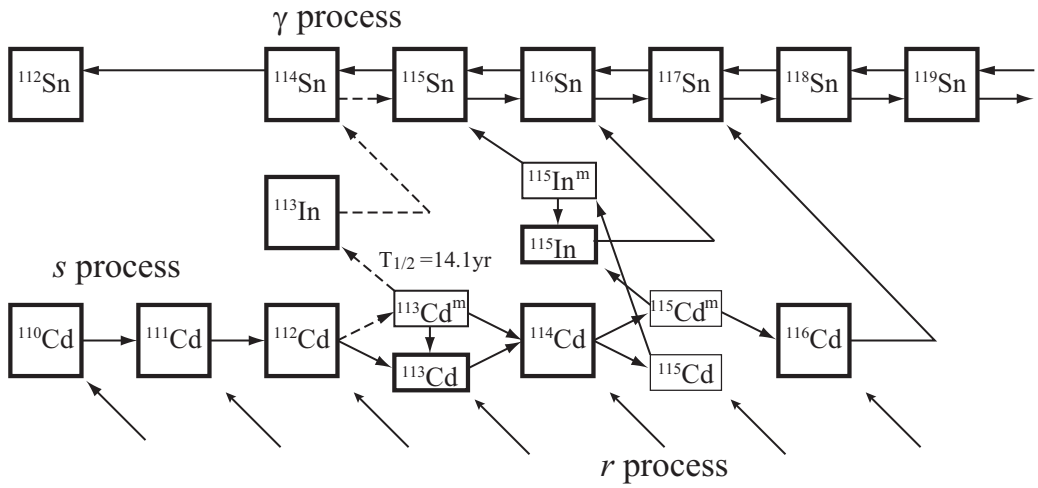

FIG. 1. Partial nuclear chart and nucleosynthesis flows around ^{113}Cd and ^{115}Sn. Most isotopes are synthesized by the *s* and *r* processes. Neutron deficient isotopes are also produced by the γ process. The isotopes of ^{112,114,115}Sn locate outside of the main *s*-process flow and shielded against β^- decay after the freeze-out of the *r* process. The dashed line shows a weak path of the *s* process from the ^{113}Cd isomer to ^{115}Sn.

neutron beams provided at the Materials and Life Science Experimental Facility (MLF) in the Japan Proton Accelerator Research Complex (J-PARC). The neutron capture γ rays were measured using a high-purity germanium (HPGe) detector system coupled with a time-of-flight (TOF) method.

II. EXPERIMENTAL PROCEDURE

The experiment was performed using the Accurate Neutron-Nucleus Reaction Measurement Instrument (ANNRI) installed at a neutron beam line, BL04, at the MLF in J-PARC. The details of the ANNRI were described in previous papers [13,14]. High flux pulsed neutrons were generated by spallation reactions on the mercury target with high energy

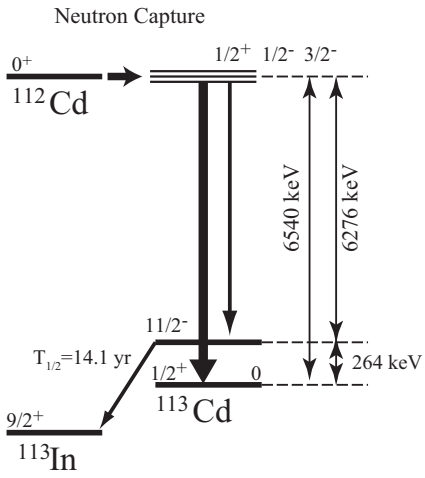

FIG. 2. Schematic view of the ^{112}Cd$(n,\gamma)^{113}$Cd reaction. Low spin excited states in ^{113}Cd are populated by neutron capture reactions on the 0^+ ground state of ^{112}Cd. Each populated state decays away to the ground state or the isomer. The energy difference between the maximum γ ray and the γ ray decaying to the isomer is only 264 keV.

proton beams. The proton beams with an energy of 3 GeV were injected into the mercury target at a repetition rate of 25 Hz. The average beam power was 200 kW. The proton beam was operated with a double bunch mode; a single proton beam pulse includes two proton bunches with widths of 100 ns and the time interval between the two bunches is 600 ns. A lead absorber with a thickness of 37.5 mm was located downstream from the neutron source to absorb prompt γ rays generated by spallation reactions. The ANNRI has an HPGe detector array, which consists of two cluster HPGe detectors, eight coaxial HPGe detectors, and bismuth germanate (BGO) Compton-suppression detectors. This detector array was located 21.5 m downstream from the neutron source. A ^{112}Cd foil enriched to 98.27% was set at the center of the detector array. Since the neutron beam collimator with a diameter of 7 mm was located upstream from the target position, the diameter of the neutron beam on the target is 7 mm. In the present experiment, we used the two cluster HPGe detectors with BGO Compton-suppression detectors. Individual cluster detectors have seven HPGe crystals. The energies of neutrons were measured using a TOF method by recording the time when the detectors measured the γ rays from the target. When at least one crystal detected a γ ray, the energies of γ rays measured by all crystals and the time when the detector was fired were recorded event by event in a list mode.

III. RESULT AND DISCUSSION

The ^{112}Cd$(n,\gamma)^{113}$Cd^{gs} reaction cross section at the thermal energy has not been reported. Thus, the isomer production ratio at the thermal energy has not been obtained. In 1966, Baldock *et al.* [15] measured the cross section of 2.2 barn as an effective neutron capture cross section due to both thermal and epithermal neutrons provided from a nuclear reactor. Vertebniy *et al.* [16] reported a value of 0.5 barn as an upper limit of the thermal neutron capture cross section. Thus, the measurement of the capture cross section at the thermal energy

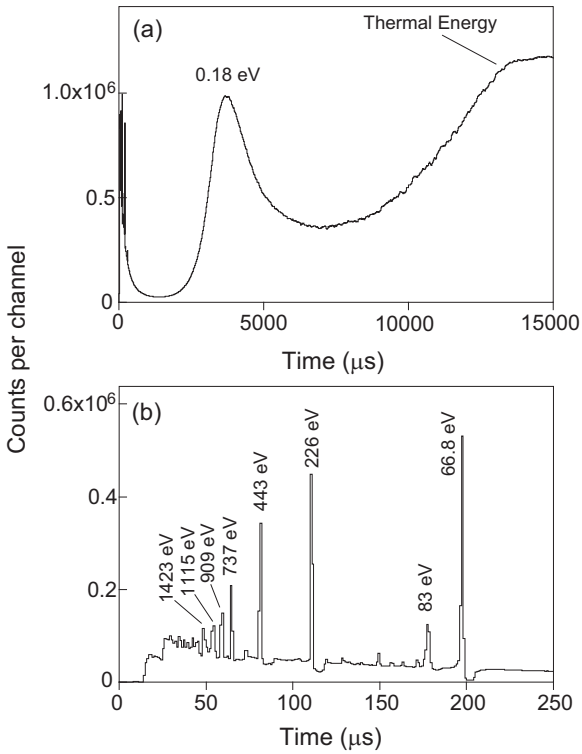

FIG. 3. TOF spectra in the thermal energy region (a) and the energy region from eV to keV (b). The large peak at the thermal energy originate from the contamination of ^{113}Cd to the enriched ^{112}Cd target. The neutron capture resonance on ^{113}Cd at 0.18 eV is also observed. In an energy region higher than the thermal energy, the resonances on ^{112}Cd are clearly observed.

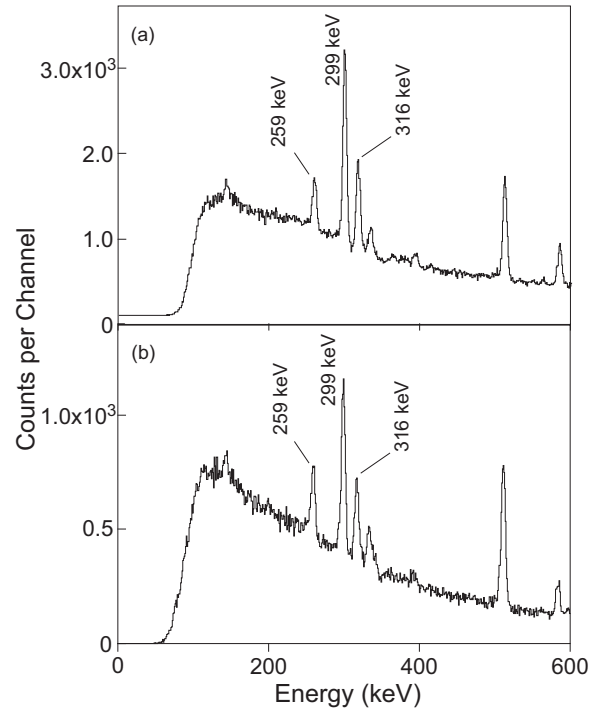

FIG. 4. The γ-ray energy spectra measured by the two cluster type of HPGe detectors. (a) Gated spectrum by neutron energy of 66.8 eV. (b) Gated spectrum by neutron energy of 737 eV. The γ rays decaying to the ground state of ^{112}Cd are observed at 299 and 316 keV. The γ ray to the isomer is also observed at 259 keV.

has been expected. Figure 3 shows TOF spectra. A large peak at 0.18 eV and the enhancement of the cross section at the thermal energy are observed [see Fig. 3(a)]. They are inferred to originate from the contamination of ^{113}Cd to the enriched ^{112}Cd target, although the fraction of ^{113}Cd is only 0.6%. The thermal neutron capture cross section of ^{113}Cd is 20615 barn [17], whereas that of ^{112}Cd is lower than 0.5 barn as discussed above. By multiplying each fraction by its cross section, the contribution of ^{112}Cd is lower than that of ^{113}Cd by more than two orders of magnitude in the present experiment. Thus, we cannot obtain the cross section of the ^{112}Cd$(n,\gamma)^{113}$Cd^{gs} reaction at the thermal energy. In contrast, it is expected that the ^{112}Cd$(n,\gamma)^{113}$Cd reaction is dominant in an energy region higher than the thermal energy. As shown in Fig. 3(b), neutron capture resonances on ^{112}Cd are clearly observed in this energy region. The energies of the measured resonances are consistent with the previous data [17]. Figure 4 shows γ-ray energy spectra with the gate on 66.8 and 737 eV neutron energies in the TOF. The γ rays decaying to the ground state of ^{113}Cd with energies of 299 and 316 keV are clearly observed in both spectra. A γ ray of 259 keV which decays to the isomer is also observed. The γ rays observed in the present experiment are indicated by the solid arrows in the partial level scheme of ^{113}Cd (see Fig. 5).

Hayakawa *et al.* [6] measured only the thermal neutron capture cross section to the ^{113}Cd isomer using neutrons provided from a nuclear reactor and calculated the *s*-process contribution from the ^{113}Cd isomer to the solar abundance of ^{115}Sn using a classical steady flow model. The *s*-process

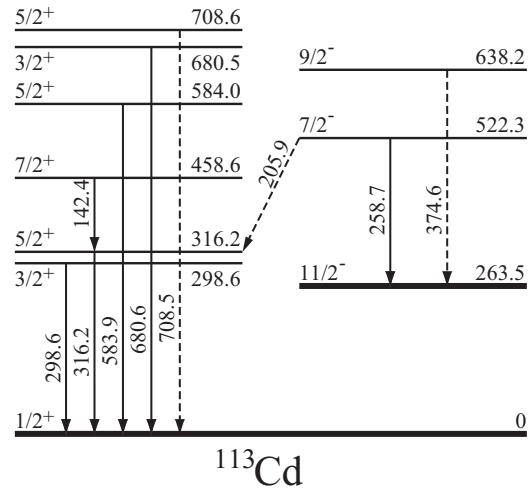

FIG. 5. Partial level scheme of ^{113}Cd. There is the ground state with $J^\pi = 1/2^+$ and the isomer with $J^\pi = 11/2^-$. The branching ratio to the isomer depends on the spin and parity of states populated by neutron capture reactions. The solid arrows are the γ transitions observed in the present experiment. The dashed arrows indicate unobserved γ rays.

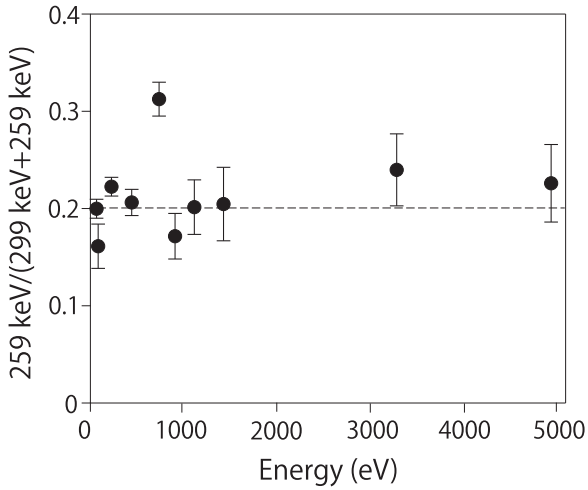

FIG. 6. Measured γ-ray intensity ratios of 259 keV to the sum of 299 and 259 keV. These ratios are expected to be approximately proportional to the isomer production ratios. The ratios for the measured resonances are almost constant except the ratio at 737 eV. These resonances are assigned to the s-wave neutron capture resonances.

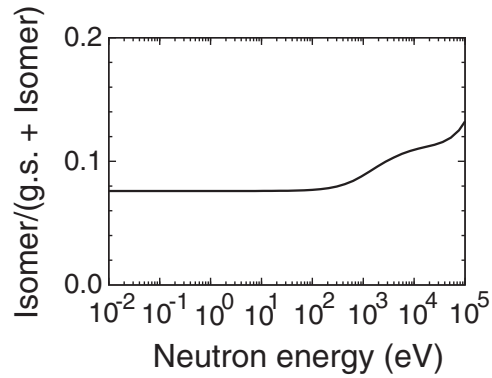

FIG. 7. Calculated isomer production ratios following the ^{112}Cd$(n,\gamma)^{113}$Cd reaction. The ratio is almost constant in an energy region of $E < 100$ eV. On the other hand, in an energy region of $E > 100$ eV, the ratio increases with increasing neutron energy.

contribution depends on the isomer production ratio at s-process related energies of $E \sim$ 1–50 keV. The ratios in this energy region were calculated by using a statistical model. If the ratio increases in an energy region higher than keV, the origin of ^{115}Sn may be explained by the s process. From the viewpoint of the statistical model, the isomer production ratio depends strongly on the spin and parity of an exited state populated by a neutron capture reaction. The $J^\pi = 1/2^+$ states are populated by s-wave neutron captures on the $J^\pi = 0^+$ ground state of ^{112}Cd (see Fig. 2). These $J^\pi = 1/2^+$ states decay strongly away to the $J^\pi = 1/2^+$ ground state of ^{113}Cd by the emission of a γ ray or cascade of γ rays, whereas the branching ratio to the $J^\pi = 11/2^-$ isomer is relatively small. The isomer branching ratio increases with increasing spin of the populated state. To evaluate the isomer production ratio as a function of neutron energy, we plot the γ ray intensity ratio of 259 keV to the sum of 259 and 299 keV, 259 keV/(299 + 259 keV), for the γ-ray spectrum with the gate on each neutron resonance energy in Fig. 6, where the dashed line is a guideline of 0.2. These ratios are assumed to be approximately proportional to the absolute isomer production ratios. It is clear that most ratios except 737 eV in an energy region of $E < 5$ keV are almost constant around the value of 0.2 (see Fig. 6). This result suggests that the isomer production ratio does not increase drastically in the energy region of $E <$ 5 keV and supports the previous result [6] that the s-process contribution from the ^{113}Cd isomer to the solar abundance of ^{115}Sn is minor. Note that the origin of ^{115}Sn may be explained by the s process if it will be found experimentally that the isomer ratio increases suddenly over 5 keV.

The isomer ratios of most resonances are almost constant as discussed above. These resonances can be explained by the decay from $J^\pi = 1/2^+$ states populated by s-wave resonances. These resonances except the 83 eV resonance were assigned to be s-wave resonances [18] by using Bayes's theorem analysis [19]. Although the weak 83 eV was assigned to a p-wave capture [18], the present result suggests that this resonance may be an s-wave resonance with $J^\pi = 1/2^+$ or a p-wave resonance with $J^\pi = 1/2^-$. The enhancement of the isomer ratio at 737 eV suggests that the spin at 737 eV is higher than or equal to 3/2. Therefore, this level can be assigned to a $J^\pi = 3/2^-$ state populated by a p-wave capture.

The neutron capture cross section on ^{112}Cd is calculated by using the CCONE code [20], in which the Hauser-Feshbach statistical model is implemented. The neutron transmission coefficient is derived by the coupled-channels optical model with the potential form [21]. The potential parameters are fixed so as to reproduce measured data of the total cross section and elastic scattering angular distributions for natural Cd. The ground state of ^{112}Cd is coupled with the $J^\pi = 2^+$, 4^+, and 6^+ levels in the yrast band by adopting quadrupole and hexadecapole deformation parameters of 0.151 and -0.028, respectively. The levels with excitation energies of up to 1192 keV in ^{113}Cd are adopted from the RIPL-3 database [22]. The states above 1192 keV, which are assumed to be continuous, are represented by the composite level density formula [23]. The γ-ray radiations of $E1$, $M1$, and $E2$ transitions are taken into account. The generalized Lorentzian model is adopted for the $E1$ strength function. The neutron capture cross section is normalized to fit to measured data in the keV energy region [5]. The calculated isomer production ratio as a function of neutron energy is shown in Fig. 7. The ratio is almost constant in a neutron energy region lower than 100 eV, whereas above 100 eV the ratio increases with increasing neutron energy. Figure 8 shows the calculated 259 keV/(299 + 259 keV) ratios of decay γ rays from populated states with $J^\pi = 1/2^+$, $1/2^-$, $3/2^+$, $3/2^-$, and $5/2^+$ following neutron capture reactions. The ratios for $J^\pi = 3/2^-$ states populated by p-wave neutron captures are about 1.6 times larger than those for $J^\pi = 1/2^+$. The measured ratio at 737 eV is larger than the ratios of the $J^\pi = 1/2^+$ states by a factor of 1.5 ± 0.1 (see Fig. 6). This agreement is consistent with the $J^\pi = 3/2^-$ assignment for 737 eV.

If the resonance at 737 eV is the p-wave resonance, the reduced neutron resonance width of 737 eV is as large

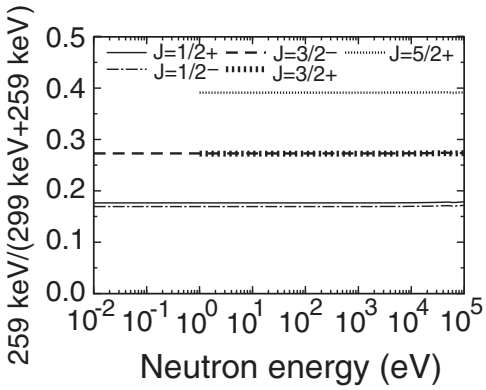

FIG. 8. Calculated production ratio of 259 keV decay γ ray to the summation of 259 and 299 keV from states with $J^\pi = 1/2^+$, $1/2^-$, $3/2^+$, $3/2^-$, and $5/2^+$ following the ^{112}Cd$(n,\gamma)^{113}$Cd reaction. The ratio from the state with $J^\pi = 3/2^-$ is about 1.6 times larger than that with $J^\pi = 1/2^+$.

as $g\Gamma_n^1 = 7.8$ eV which is calculated using the value of $g\Gamma_n = 380$ meV [17], where Γ_n and Γ_n^1 are the neutron width and the reduced neutron width for $l = 1$ resonances (p-wave capture), respectively, and g is the spin factor. It is considered that the distribution of the reduced neutron width of a partial wave neutron capture resonance follows the Porter-Thomas (PT) distribution [24]. The number of the neutron capture resonances decreases with increasing the reduced neutron width in the strong resonance region. In a mass region of $A = 100$–120 [17], there are large values of $g\Gamma_n^1 = 3.1$ eV (3429 eV resonance in ^{102}Ru), 2.2 eV (17184 eV in ^{120}Sn), 10.7 eV (2380 eV in ^{124}Sn). Thus, $g\Gamma_n^1 = 7.8$ eV is not extremely large compared with these measured widths.

There are experimental techniques to measure precisely the spin and parity of the resonance state, for example, measurements of angular distribution of neutron capture γ rays [25] and a method using polarized neutron beam [26]. The present result suggests that measurements of the isomer production ratios using HPGe detectors in conjunction with a TOF method are effective for the spin and parity assignments for neutron capture resonances in the case that the difference between the spins of the ground state and an isomer in a nucleus is larger than or equal to $\Delta J = 5$.

IV. SUMMARY

The astrophysical origin of ^{115}Sn remains an open question. An isomer with a half-life of 14.1 yr in ^{113}Cd is a branching point from which a nucleosynthesis flow reaches to ^{115}Sn. The s-process abundance of ^{115}Sn depends on the isomer production ratio in the ^{112}Cd$(n,\gamma)^{113}$Cd reaction. We measured γ rays following neutron capture reactions on ^{112}Cd using HPGe detectors in conjunction with a TOF method at the MLF in the J-PARC. In a neutron energy region higher than the thermal energy, we observed both γ rays decaying to the ground state and the isomer. The relative isomer production ratios except 737 eV are almost constant in a neutron energy region of $E < 5$ keV. This result supports the conclusion that the contribution of the s-process from the ^{113}Cd isomer to the solar abundance of ^{115}Sn is minor in the previous study [6]. The enhancement at 737 eV can be explained by the decay from a $J^\pi = 3/2^-$ state populated by a p-wave neutron capture. The isomer production ratios calculated by a statistical model support this assignment. This result suggests that measurements of isomer production ratios using HPGe detectors coupled with a TOF method is effective to assign the spin and parity of neutron capture resonances.

ACKNOWLEDGMENT

This work was supported by JSPS KAKENHI Grant No. 15H03665.

[1] R. A. Ward and H. Beer, Astrophys. Astron. **103**, 189A (1981).
[2] Zs. Németh, F. Käppeler, C. Theis, T. Belgya, and S. S. W. Yates, Astrophys. J. **426**, 357 (1994).
[3] K. Wisshak, F. Voss, C. Theis, F. Käppeler, K. Guber, L. Kazakov, N. Kornilov, and G. Reffo, Phys. Rev. C **54**, 1451 (1996).
[4] Ch. Theis *et al.*, Astrophys. J. **500**, 1039 (1998).
[5] K. Wisshak, F. Voss, F. Käppeler, and L. Kazakov, Phys. Rev. C **66**, 025801 (2002).
[6] T. Hayakawa *et al.*, Astrophys. J. **707**, 859 (2009).
[7] S. E. Woosley and W. M. Howard, Astrophys. J. Suppl. **36**, 285 (1978).
[8] M. Rayet, M. Arnould, M. Hashimoto, N. Prantzos, and K. Nomoto, Astron. Astrophys. **298**, 517 (1995).
[9] T. Hayakawa *et al.*, Astrophys. J. **685**, 1089 (2008).
[10] K. Volev *et al.*, Nucl. Instrum. Methods Phys. Res., Sect. B **300**, 11 (2013).
[11] G. Rusev, M. Jandel, M. Krtička, T. A. Bredeweg, A. Couture, T. N. Taddeucci, and J. L. Ullmann, Phys. Rev. C **87**, 054603 (2013).
[12] R. Massarczyk, G. Schramm, T. Belgya, R. Schwengner, R. Beyer, D. Bemmerer, Z. Elekes, E. Grosse, R. Hannaske, A. R. Junghans, Z. Kis, T. Kogler, C. Lorenz, K. Schmidt, L. Szentmiklosi, A. Wagner, and J. L. Weil, Phys. Rev. C **93**, 014301 (2016).
[13] K. Kino *et al.*, Nucl. Instrum. Methods Phys. Res., Sect. A **736**, 66 (2014).
[14] T. Katabuchi, T. Matsuhashi, K. Terada, M. Igashira, M. Mizumoto, K. Hirose, A. Kimura, N. Iwamoto, K. Y. Hara, H. Harada, J.-I. Hori, T. Kamiyama, K. Kino, F. Kitatani, Y. Kiyanagi, S. Nakamura, and Y. Toh, Phys. Rev. C **91**, 037603 (2015).
[15] C. R. Baldock, J. Halperin, L. E. Idom, and J. H. Oliver, Oak Ridge National Laboratory Report No. 3994, 1966 (unpublished).
[16] V. P. Vertebniy *et al.*, Yad. Fiz. Issl. **6**, 115 (1968).
[17] S. F. Mughabghab, *Atlas of Neutron Resonances, Resonance Parameters and Thermal Cross Sections* $Z = 1$–100 (Elsevier Science, Amsterdam, 2006).
[18] H. I. Liou *et al.*, Phys. Rev. C **10**, 709 (1974).

[19] H. I. Liou *et al.*, Phys. Rev. C **5**, 974 (1972).
[20] O. Iwamoto *et al.*, Nucl. Data Sheets **131**, 259 (2016).
[21] S. Kunieda *et al.*, J. Nucl. Sci. Technol. **44**, 838 (2007).
[22] R. Capote *et al.*, Nucl. Data Sheets **110**, 3107 (2009).
[23] A. Gilbert, A. G. W. Cameron, Can. J. Phys. **43**, 1446 (1965).
[24] C. E. Poter and R. G. Thomas, Phys. Rev. **104**, 483 (1956).
[25] M. R. Bhat, R. E. Chrien, O. A. Wasson, M. Beer, and M. A. Lone, Phys. Rev. **166**, 1111 (1967).
[26] Hans Postma, H. Marshak, V. L. Sailor, F. J. Shore, and C. A. Reynolds, Phys. Rev. **126**, 979 (1962).